MYB20, MYB42, MYB43, and MYB85 Regulate Phenylalanine and Lignin Biosynthesis during Secondary Cell Wall Formation[1][OPEN]

Pan Geng,[a] Su Zhang,[a,b] Jinyue Liu,[a] Cuihuan Zhao,[a] Jie Wu,[a,b] Yingping Cao,[c] Chunxiang Fu,[c] Xue Han,[d] Hang He,[d] and Qiao Zhao[a,2,3]

[a]Center for Plant Biology, School of Life Sciences, Tsinghua University, Beijing 100084, China
[b]Tsinghua University-Peking University, Joint Center for Life Sciences, Beijing 100084, China
[c]Shandong Technology Innovation Center of Synthetic Biology, Key Laboratory of Biofuels, Qingdao Institute of Bioenergy and Bioprocess Technology, Chinese Academy of Sciences, Qingdao, Shandong, 266101, China
[d]State Key Laboratory of Protein and Plant Gene Research, Peking-Tsinghua Center for Life Sciences, School of Advanced Agriculture Sciences and School of Life Sciences, Peking University, 100871 Beijing, China

ORCID IDs: 0000-0002-0946-005X (P.G.); 0000-0003-3165-283X (H.H.); 0000-0002-0958-4300 (Q.Z.).

Lignin is a phenylpropanoid-derived polymer that functions as a major component of cell walls in plant vascular tissues. Biosynthesis of the aromatic amino acid Phe provides precursors for many secondary metabolites, including lignins and flavonoids. Here, we discovered that MYB transcription factors MYB20, MYB42, MYB43, and MYB85 are transcriptional regulators that directly activate lignin biosynthesis genes and Phe biosynthesis genes during secondary wall formation in Arabidopsis (*Arabidopsis thaliana*). Disruption of *MYB20*, *MYB42*, *MYB43*, and *MYB85* resulted in growth development defects and substantial reductions in lignin biosynthesis. In addition, our data showed that these MYB proteins directly activated transcriptional repressors that specifically inhibit flavonoid biosynthesis, which competes with lignin biosynthesis for Phe precursors. Together, our results provide important insights into the molecular framework for the lignin biosynthesis pathway.

Plant cell walls are commonly classified into primary and secondary based on their composition and cellular location. In general, all plant cells form primary cell walls during cell division, while secondary cell walls are produced after cessation of cell division and expansion only in specific types of cells, such as vessel elements and fibers (Cosgrove and Jarvis, 2012). Secondary cell walls play important roles in providing long-distance water transport, mechanical support, and plant defense (Zhao and Dixon, 2014; Hoson and Wakabayashi, 2015).

The main components of typical secondary cell walls are cellulose, hemicellulose, and lignin. Lignins are phenylpropanoid-derived polymers resulting from oxidative polymerization of three major hydroxycinnamyl alcohols (Bonawitz and Chapple, 2010; Zhao, 2016). Natural lignin polymers are only composed of *p*-hydroxyphenyl, guaiacyl, and syringyl as basic units; however, occasionally some unconventional units, such as coniferaldehyde, sinapaldehyde, catechyl, and 5-hydroxyl guaiacyl units, are also incorporated into lignin monomers (Weng et al., 2010; Chen et al., 2012, 2013; Zhao et al., 2013).

It is widely accepted that lignin biosynthesis is controlled by a regulatory hierarchy involving NAC (no apical meristem [NAM], Arabidopsis transcription activation factor [ATAF1/2], and cup-shaped cotyledon [CUC2]) and myeloblastosis (MYB) transcription factors (Zhao, 2016; Ohtani and Demura, 2019). In this network, NAC proteins, including VASCULAR-RELATED NAC DOMAIN1 (VND1) to VND7 and NAC SECONDARY WALL THICKNING PROMOTING FACTOR1 (NST1) to NST3 were identified in Arabidopsis (*Arabidopsis thaliana*) to serve as a first layer of transcription factors (Kubo et al., 2005; Mitsuda et al., 2007). These NACs are master regulators in various cell types. NST3, also called SND1, together with NST1 redundantly regulates secondary cell wall formation in fibers (Mitsuda et al., 2007), and NST1 and NST2 activate the same process in the endothecium of anthers (Mitsuda et al., 2005). MYB46 and MYB83 in Arabidopsis, the downstream

[1]This work was supported by the Youth Thousand Scholar Program of China (grant no. 31522008), the National Natural Science Foundation of China (grant no. 31570296), and the School of Life Sciences, Tsinghua University.

[2]Author for contact: qzhao@mail.tsinghua.edu.cn.
[3]Senior author.
The author responsible for distribution of materials integral to the findings presented in this article in accordance with the policy described in the Instructions for Authors (www.plantphysiol.org) is: Qiao Zhao (qzhao@mail.tsinghua.edu.cn).

P.G. and Q.Z. designed the research; P.G., S.Z., J.L., C.Z., J.W., Y.C., X.H., H.H., and C.F. performed the experiments; P.G. and Q.Z. wrote the article.
[OPEN]Articles can be viewed without a subscription.
www.plantphysiol.org/cgi/doi/10.1104/pp.19.01070

targets of the NAC proteins, are a second layer of the network, redundantly regulating secondary cell wall formation (McCarthy et al., 2009; Ko et al., 2014). Recently, two types of cis-element sequences were reported by two different groups, secondary wall MYB-responsive element, ACC(A/T)A(A/C)(T/C), and MYB46-responsive cis-regulatory element, (T/C)ACC(A/T)A(A/C)(T/C) (Kim et al., 2012; Zhong and Ye, 2012). Comprehensive survey of these cis-elements and DNA protein-binding assays identified the direct targets of MYB46/83, including *MYB* genes implicated in the regulation of lignin biosynthesis (e.g. *MYB58*, *MYB63*, *MYB103*, and *KNAT7*), secondary cell wall biosynthesis genes such as cellulose synthase genes (*CesA4*, *CesA7*, and *CesA8*), xylan biosynthesis genes (*IRX7*, *IRX8*, and *IRX9*), and lignin biosynthesis genes (*PAL1*, *C4H*, *4CL1*, *CCoAOMT*, *HCT*, *CCR1*, and *F5H1*; Kim et al., 2012, 2013a, 2013b, 2014; Wang et al., 2020a).

It was previously revealed that the majority of promoters of lignin biosynthesis genes contain so-called AC elements, including AC-I (ACCTACC), AC-II (ACCAACC), and AC-III (ACCTAAC), that are recognized by transcription factors (Raes et al., 2003). MYB58 and MYB63 were shown to activate lignin biosynthesis genes by directly targeting the AC elements in Arabidopsis (Zhou et al., 2009). Members from subfamily 4 of the R2R3-MYB family can also target the AC elements to function as transcriptional repressors of the lignin biosynthesis pathway. AmMYB308 and AmMYB330 in *Antirrhinum majus*, EgMYB1 and EgMYB2 in *Eucalyptus gunnii*, PtMYB1, PtMYB4, PtMYB8, and PtMYB14 in *Pinus teada*, PgMYB1, PgMYB8, PgMYB14, and PgMYB15 in *Picea glauca*, ZmMYB31 and ZmMYB42 in maize (*Zea mays*), and Arabidopsis MYB4, MYB32, and MYB75 were all reported to directly regulate lignin biosynthesis genes (Tamagnone et al., 1998; Jin et al., 2000; Patzlaff et al., 2003; Preston et al., 2004; Goicoechea et al., 2005; Bhargava et al., 2010; Fornalé et al., 2010; Legay et al., 2010; Bomal et al., 2014).

The synthesis of lignin monomers involves the phenylpropanoid pathway, which is also shared by many other metabolites such as suberin, flavonoids, tannins, and lignans (Fraser and Chapple, 2011). The aromatic amino acid Phe, the end product of the shikimate pathway, serves as the precursor of downstream phenylpropanoids (Maeda and Dudareva, 2012; Tohge et al., 2013). Lignin biosynthesis is a high-energy-consuming and irreversible process; therefore, it is critical that lignin deposition is tightly controlled to avoid overconsumption of Phe. Transcription factors have been identified that coordinately regulate the expression of Phe biosynthesis and the downstream metabolism of Phe. Ectopic expression of the petunia (*Petunia hybrida*) transcription factor ODORANT1 (ODO1) in tomato (*Solanum lycopersicum*) can induce shikimate biosynthesis genes and phenylpropanoid-associated genes (Dal Cin et al., 2011). Green tea (*Camellia sinensis*) MYB4 negatively regulates phenylpropanoid and shikimate biosynthesis by directly targeting the AC elements of promoters of the genes involved in the two pathways (Li et al., 2017).

L-Phe is an aromatic amino acid required not only for protein biosynthesis but also for many secondary metabolites, such as flavonoids, condensed tannins, lignans, and lignins (Maeda and Dudareva, 2012). In plants, Phe is produced by two alternative pathways. Most Phe is produced via the chloroplast-localized arogenate pathway (Maeda et al., 2010). In addition, a cytosolic postchorismate Phe biosynthesis pathway has also been functionally characterized (Yoo et al., 2013; Qian et al., 2019). It was proposed that the alternative cytosolic pathway may contribute to produce specialized Phe-derived metabolites in response to biotic and abiotic stress in plants (Qian et al., 2019).

MYB20, *MYB42*, *MYB43*, and *MYB85* were previously identified as secondary cell wall-related transcription factors based on a genome-wide transcriptome analysis of NST1 down-regulated mutants in Arabidopsis (Zhong et al., 2008). Dominant repression of MYB85, which is a transcriptional activator, substantially reduced secondary wall thickening in fiber cells, and overexpression of MYB85 caused ectopic deposition of lignin in epidermal and cortical cells in stems. However, how these MYBs are involved in secondary cell wall formation remains elusive. In this study, we report that MYB20, MYB42, MYB43, and MYB85 redundantly activate both Phe and lignin biosynthesis. In addition, MYB20, MYB42, MYB43, and MYB85 activate the transcription factor *MYB4*, which represses flavonoid biosynthesis to optimize Phe flux to the lignin biosynthesis pathway. This discovery uncovers another level of complexity in the regulatory network of plant lignin biosynthesis.

RESULTS

MYB20, *MYB42*, *MYB43*, and *MYB85* Genes Are Regulated by NST3 and MYB46

It was previously revealed that several unknown transcription factors are under the control of SND1 and NST1, including two NACs (*SND2* and *SND3*) and eight MYB genes (*MYB20*, *MYB42*, *MYB43*, *MYB52*, *MYB54*, *MYB69*, *MYB85*, and *MYB103*; Zhong et al., 2008). Phylogenetic analysis demonstrated that MYB42 and MYB85 are closely related to each other, while MYB20 and MYB43 are likely more closely related to one another (Supplemental Fig. S1). Furthermore, the two subgroups are also closely related, but they are remotely related to the previously reported lignin transcriptional activators MYB58 and MYB63 (Supplemental Fig. S1). Therefore, we selected MYB20, MYB42, MYB43, and MYB85 to functionally characterize their roles in secondary cell wall biosynthesis. Consistent with the fact that *MYB20*, *MYB42*, *MYB43*, and *MYB85* are regulated by NST3, the transcript levels of all four MYB genes were reduced in the double mutant *nst1/3* (Fig. 1A). MYB46, which is a direct target of NST3, is also a master regulator of secondary cell wall biosynthesis, potentially controlling

the expression of *MYB20*, *MYB42*, *MYB43*, and *MYB85*. To determine whether MYB46 and NST3 can activate *MYB20*, *MYB42*, *MYB43*, and *MYB85* transcription, we performed transient expression assays in *Nicotiana benthamiana* leaves. The promoters of *MYB20*, *MYB42*, *MYB43*, and *MYB85* were fused with *Luciferase* (*LUC*) to generate P_{MYB20}-*LUC*, P_{MYB42}-*LUC*, P_{MYB43}-*LUC*, and P_{MYB85}-*LUC*, respectively. MYB46 and NST3 were driven by the 35S promoter to act as effectors. Coexpression of MYB46 or NST3 can activate P_{MYB20}-*LUC*, P_{MYB42}-*LUC*, P_{MYB43}-*LUC*, and P_{MYB85}-*LUC* activity (Fig. 1, B and C). However, neither NST1 to NST3 nor MYB46 and MYB83 were able to bind these promoters in yeast one-hybrid assays (Supplemental Fig. S2).

Simultaneous Disruption of *MYB20*, *MYB42*, *MYB43*, and *MYB85* Causes Plant Growth Defects

To further investigate the functions of these genes, the T-DNA insertion lines of *myb20-1* (GK-109C11-012312), *myb42-1* (SALKseq_78190.1), *myb43-1* (SALK_085312), and *myb85-1* (SALK_052089) were characterized and the insertion positions were verified by genomic sequencing (Fig. 1D). Reverse transcription PCR showed that these T-DNA insertion lines were null mutants (Fig. 1E). The double mutants *myb20/43* and *myb42/85* exhibited a normal growth phenotype, similar to the wild type (Fig. 2A). However, the quadruple mutant *myb20/42/43/85* showed a semidwarfism phenotype compared with *myb20/43* and *myb42/85*, indicating genetic redundancy among these genes (Fig. 2A). In addition, the quadruple mutant also showed shorter siliques with compromised fertility (Fig. 2, B–D).

MYB20, MYB42, MYB43, and MYB85 Coordinately Regulate Phe and Lignin Biosynthesis

To determine the possible effects on gene expression of disrupting *MYB20*, *MYB42*, *MYB43*, and *MYB85*, we used high-throughput mRNA sequencing to identify differentially expressed genes in the quadruple mutant *myb20/42/43/85* compared with wild-type plants. In the quadruple mutant *myb20/42/43/85*, a total of 2,596 genes were expressed at levels significantly different from the wild type (Supplemental Data Sets S1 and S2). Kyoto Encyclopedia of Genes and Genomes (KEGG) pathway analysis showed that biosynthesis of secondary metabolites was changed greatly (Supplemental Fig. S3) and genes involved in lignin and Phe biosynthesis showed reduced expression in the quadruple mutant. To further verify the RNA sequencing data, we performed RT-qPCR to compare gene expression among the double mutants *myb20/43* and *myb42/85*, the quadruple mutant *myb20/42/43/85*, and the wild type. *myb20/42/43/85* plants exhibited reduced transcript levels of lignin biosynthesis genes such as *PAL1*, *4CL1*, *C4H*, *CSE*, *HCT*, and *CAD4*, while the reduction was less severe in both double mutants (Fig. 3B). The transcript levels of *ADT4*, *ADT5*, and *ADT6*, which are specifically involved in Phe

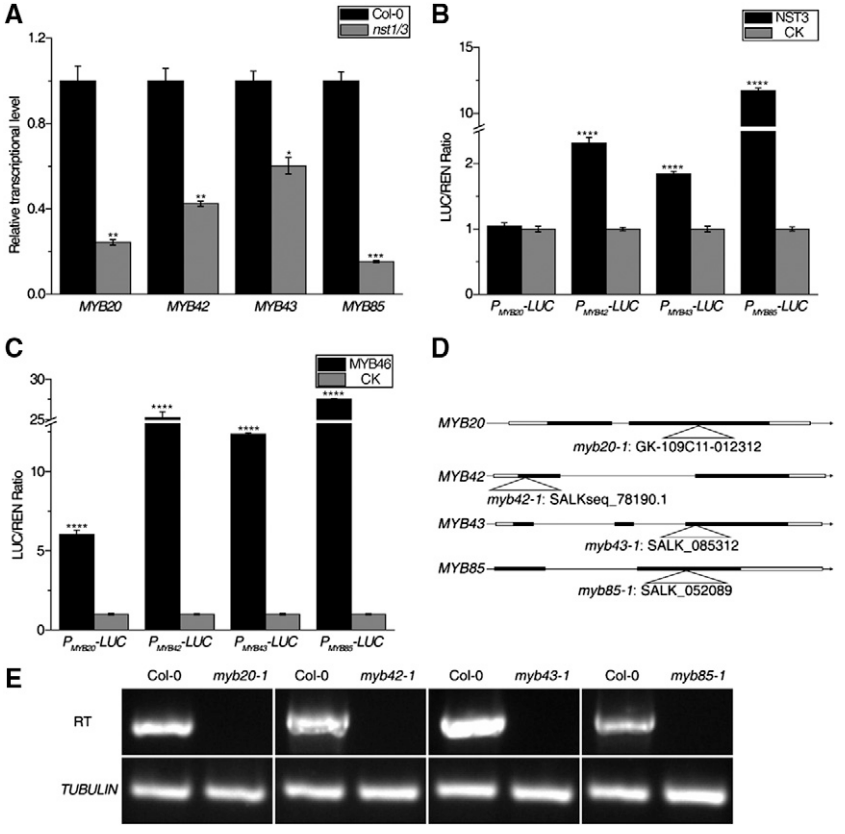

Figure 1. Description of *myb20*, *myb42*, *myb43*, and *myb85* mutants. A, Relative transcript levels of *MYB20*, *MYB42*, *MYB43*, and *MYB85* in the inflorescence stems of 33-d-old wild-type (Columbia-0 [Col-0]) and *nst1/3* mutant plants were determined by reverse transcription quantitative PCR (RT-qPCR). The expression level in Col-0 was set to 1. *Tubulin* was used as the internal control. B and C, Transient expression assays showed that the promoters of *MYB20*, *MYB42*, *MYB43*, and *MYB85* can be activated by NST3 (B) and MYB46 (C). The P_{MYB20}-*LUC*, P_{MYB42}-*LUC*, P_{MYB43}-*LUC*, and P_{MYB85}-*LUC* reporters were cotransformed with the indicated constructs in *N. benthamiana* leaves. The LUC/REN ratio represents the LUC activity relative to the REN activity. CK was the vector of GUS-pEarleyGate 101, used as a control, and was set to 1. Data are means ± SD of three biological replicates. Asterisks indicate significant differences by Student's *t* test (*, $P < 0.05$; **, $P < 0.01$; ***, $P < 0.001$; and ****, $P < 0.0001$). D, Schematic diagrams of the structures of *MYB20*, *MYB42*, *MYB43*, *MYB85*, and T-DNA insertions. Solid boxes represent exons, black lines represent introns, and hollow boxes represent untranslated regions. E, RT-PCR analysis of *MYB20*, *MYB42*, *MYB43*, and *MYB85* transcripts in the inflorescence stems of 33-d-old plants. *Tubulin* was used as a positive control.

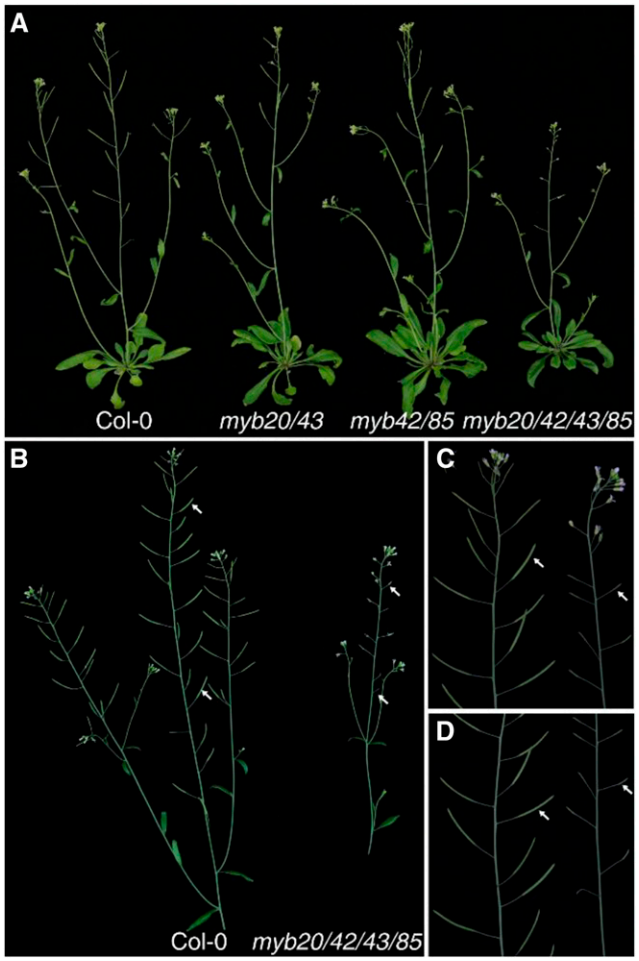

Figure 2. Disruption of *MYB20/42/43/85* causes growth and fertility defects. A, Five-week-old plants of Col-0, the double mutants *myb20/43* and *myb42/85*, and the quadruple mutant *myb20/42/43/85*. B, The inflorescence stems of 6-week-old plants of Col-0 and *myb20/42/43/85*. C, The upper inflorescence stems as in B. D, The middle inflorescence stems as in B.

biosynthesis, were greatly reduced in *myb20/42/43/85* plants but were not significantly changed in the *myb20/43* and *myb42/85* mutants, indicating genetic redundancy among the MYB genes (Fig. 3A). On the other hand, the expression of *ADH2*, *TSA1*, and *TSB1*, involved in Tyr and Trp biosynthesis, was not significantly changed in *myb20/42/43/85* mutants even though these genes are also related to the shikimate biosynthesis pathway (Fig. 3A).

The thioacidolysis method was used to determine the lignin composition of double mutants *myb20/43* and *myb42/85* and the quadruple mutant *myb20/42/43/85*. As shown in Figure 3D, the G and S subunits were significantly reduced in *myb20/42/43/85* plants, while the reduction was less severe in the two double mutants, which is consistent with the growth phenotypes and gene expression analysis (Figs. 2A and 3B). To further confirm the impact on lignin biosynthesis of disrupting *MYB20*, *MYB42*, *MYB43*, and *MYB85*, the total lignin content of mutants and control plants was quantified by Klason analysis. As shown in Supplemental Figure S4, *myb20/42/43/85* plants produced significantly reduced lignin, while double mutants *myb20/43* and *myb42/85* contained similar lignin content to wild-type plants.

Phe content was also quantified using the same mature stem tissues used for lignin measurements. Interestingly, both *myb20/43* and *myb42/85* accumulated greatly elevated levels of Phe, and *myb20/42/43/85* plants contained even more Phe than the double mutants (Fig. 3C). These results were not consistent with the fact that *ADT* genes were down-regulated in the mutants. However, the increase of the free form of Phe may be due to the reduction of downstream Phe-derived lignin biosynthesis.

MYB20, MYB42, MYB43, and MYB85 Activate Phe and Lignin Biosynthesis Gene Expression

To investigate the molecular mechanism underlying the roles of the MYB transcription factors in lignin and Phe biosynthesis pathways, a yeast one-hybrid assay was performed. We found that full-length MYB proteins had very low expression levels in the EGY48 yeast strain, but truncated MYB proteins could be easily expressed (Supplemental Fig. S5). Therefore, we used truncated proteins in the yeast one-hybrid assay. *ADT6* and *HCT* were selected as representative Phe and lignin biosynthesis genes, respectively. MYB20, MYB42, and MYB85 were able to activate the *LacZ* reporter genes driven by the *ADT6* and *HCT* promoters, while MYB43 could only activate the *LacZ* reporter gene driven by the *HCT* promoter (Figs. 4A and 5A). We utilized the electrophoretic mobility shift assay (EMSA) to further verify the direct binding to the *ADT6* and *HCT* promoters. All four recombinant MBP-MYB fusion proteins caused an upshift of the labeled *ADT6* promoter or *HCT* promoter. By contrast, MBP alone did not generate the same mobility shift (Figs. 4, C–F–F, and 5, C–F–F). The schematic diagrams of the promoters in yeast one-hybrid assays and EMSA are shown in Figures 4B and 5B.

To further confirm that MYB20, MYB42, MYB43, and MYB85 were able to activate the expression of *ADT6* and *HCT*, we performed a transient expression assay in Arabidopsis protoplasts. Coexpression of MYB20, MYB42, MYB43, or MYB85 dramatically activated P_{ADT6}-*LUC* and P_{HCT}-*LUC* activity in Arabidopsis Col-0 protoplasts (Figs. 4G and 5G). To further examine whether each MYB is able to activate the genes independently, a similar transient expression assay was carried out in Arabidopsis *myb20/42/43/85* mutant protoplasts. It turned out that each MYB was able to activate downstream targets alone (Figs. 4H and 5H), suggesting that these four MYBs are not interdependent.

MYB20, MYB42, MYB43, and MYB85 Optimize Phe Distribution in the Phenylpropanoid Biosynthesis Pathway

Our RNA sequencing data indicated that the previously identified phenylpropanoid pathway transcription

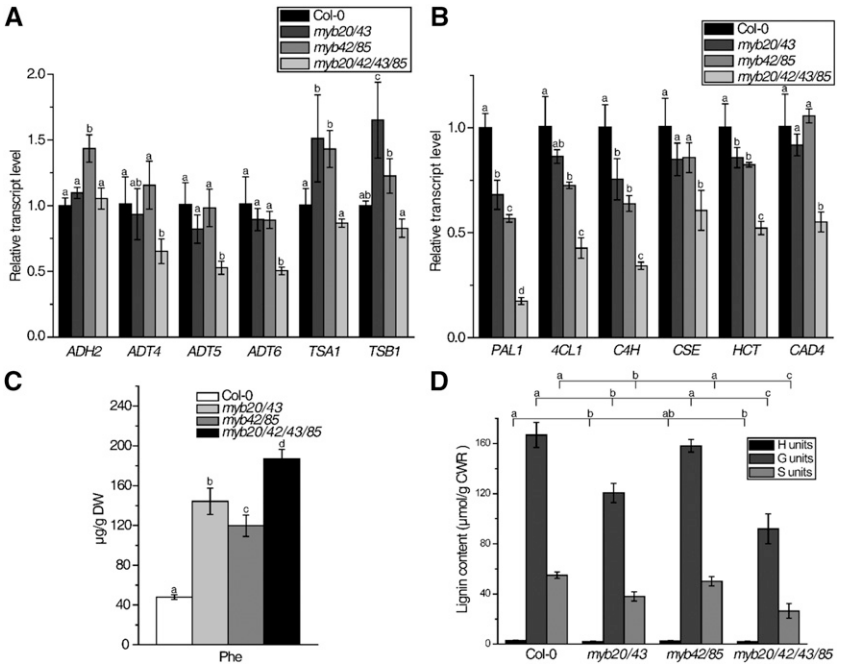

Figure 3. MYB20, MYB42, MYB43, and MYB85 redundantly regulate Phe and lignin biosynthesis. A and B, Relative transcript levels of aromatic amino acid (A) and lignin (B) biosynthesis genes in the inflorescence stems of 33-d-old Arabidopsis wild-type, *myb20/43*, *myb42/85*, and *myb20/42/43/85* mutant plants as determined by RT-qPCR. C, Phe level in the inflorescence stems of plants with the same genotypes and period as in A. DW, Dry weight. D, Lignin composition analysis of the inflorescence stems of plants with the same genotypes and period as in A. Gas chromatography (GC) quantification is shown for *p*-hydroxyphenyl (H), guaiacyl (G), and syringyl (S) lignin units by thioacidolysis. CWR, Cell wall residue. Data are means ± SD of three biological replicates. Based on Tukey's test, columns with the same letters are not significantly different and columns with different letters are significantly different ($P < 0.05$; one-way ANOVA).

factor *MYB7* was down-regulated in *myb20/42/43/85* compared with the wild type (Supplemental Data Set S2). Through RT-qPCR analysis, we showed that not only *MYB7* but also two homologous genes, *MYB4* and *MYB32*, showed lower transcript levels in the *myb20/42/43/85* mutant compared with the wild type (Fig. 6A). Transient expression assays in *N. benthamiana* leaves indicated that MYB20, MYB42, MYB43, and MYB85 activate the promoters of *MYB4* (Fig. 6B). EMSA was performed to investigate whether *MYB4* was directly targeted, as described previously (Zhao et al., 2007). EMSA showed that all four MBP-MYB proteins could bind the *MYB4* promoter but not the MBP tag (Fig. 6, C–F).

It has been reported that MYB4 can repress the expression of *Chalcone Synthase* (*CHS*), encoding the enzyme that catalyzes the first step of flavonoid biosynthesis, which competes with lignin biosynthesis for Phe as a precursor (Jin et al., 2000). Consistent with this finding, the transcript level of *CHS* was significantly enhanced in *myb20/42/43/85* compared with the wild type and was increased even more in the *myb4/7/32* mutant (Fig. 7A). These results suggest that MYB20, MYB42, MYB43, and MYB85 activate *MYB4*, *MYB7*, and *MYB32*, resulting in the down-regulation of *CHS* expression. To investigate the possible effects on the phenylpropanoid biosynthesis pathway of disrupting MYB20, MYB42, MYB43, and MYB85, we compared flavonoid accumulation among *myb20/42/43/85*, *myb4/7/32*, and wild-type plants. As shown in Figure 7B, kaempferol 3-*O*-[6′′-*O*-(rhamnosyl)glucoside] 7-*O*-rhamnoside, kaempferol 3-*O*-glucoside 7-*O*-rhamnoside, and kaempferol 3-*O*-rhamnoside 7-*O*-rhamnoside accumulated at significantly higher amounts in *myb20/42/43/85* and *myb4/7/32*. In addition, *myb20/43*, *myb42/85*, and *myb20/42/43/85* also accumulated enhanced levels of anthocyanin (Supplemental Fig. S6). These data suggest that down-regulation of the transcription repressors *MYB4*, *MYB7*, and *MYB32* in *myb20/42/43/85* leads to enhanced flavonoid biosynthesis due to elevated expression of *CHS*.

DISCUSSION

During the last decade, the transcriptional regulation of secondary cell wall formation has been extensively studied. Lignin biosynthesis has been shown to be under the control of the NAC-MYB-based transcriptional regulatory network (Ohtani and Demura, 2019). NAC proteins as master switches coordinately regulate the entirety of secondary cell wall formation, including cellulose, hemicellulose, and lignin (Zhong et al., 2010). Lignin biosynthesis is derived from the aromatic amino acid Phe, and the deposition process is believed to be irreversible. Therefore, lignin biosynthesis is not only coordinately regulated along with other secondary cell wall components but also interacts with primary metabolic pathways related to Phe biosynthesis and other branches of the phenylpropanoid pathway (Li et al., 2016; Ohtani et al., 2016).

MYB58 and MYB63 were first reported in Arabidopsis as lignin-specific transcriptional activators (Zhou et al., 2009). These MYBs are able to directly activate lignin biosynthesis genes, including early genes such as *PAL*, *C4H*, and *4CL* that are shared by other branches of the phenylpropanoid pathway such as flavonoid biosynthesis. MYB4 was shown to directly target lignin biosynthesis genes as repressors (Shen et al., 2012; Li et al., 2017). Currently, there is no

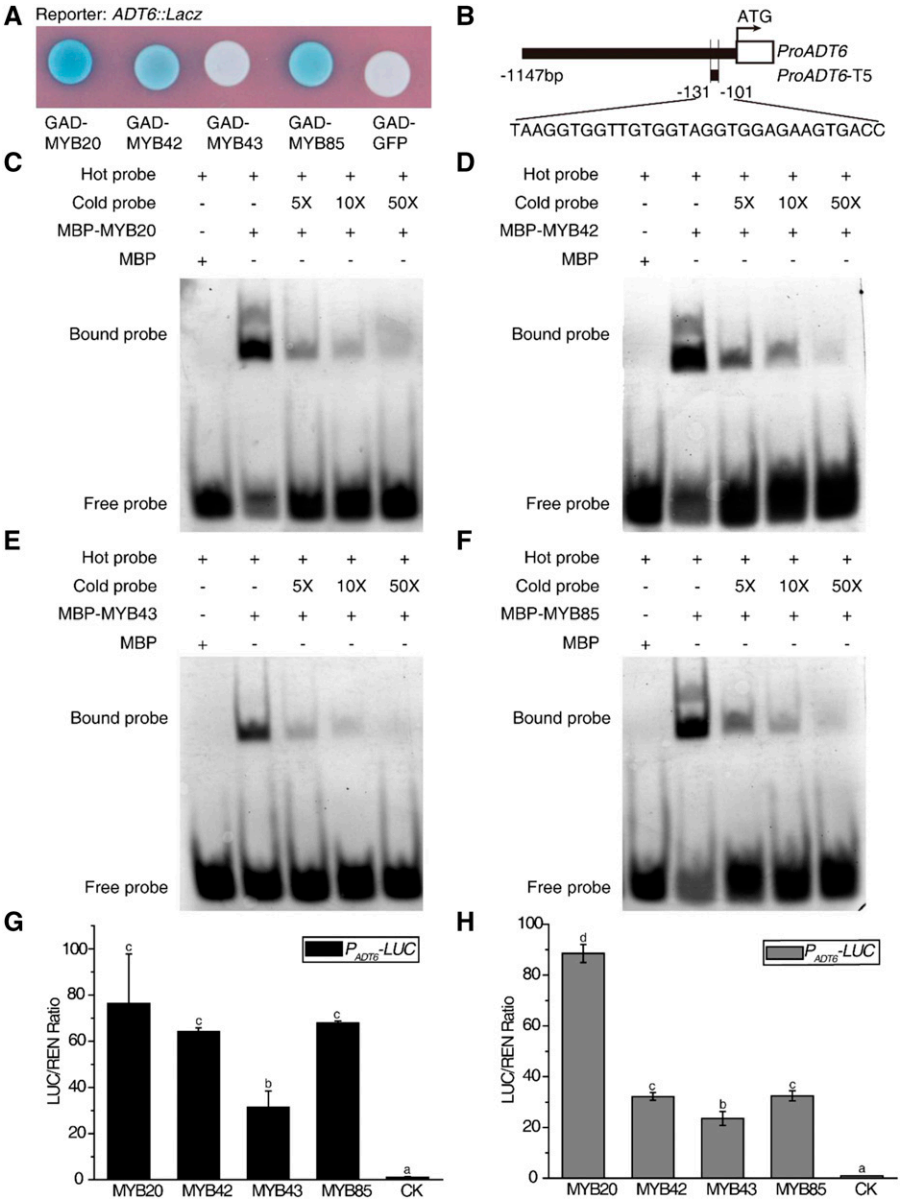

Figure 4. MYBs activate Phe biosynthesis genes. A, GAD-MYBs activate the expression of the *LacZ* reporter gene driven by the *ADT6* promoter in yeast. GFP was used as the negative control. B, The top schematic diagram and the bottom one show the promoter regions of *ADT6* in A and in C to F separately. C to F, EMSA showed that MYB20 (C), MYB42 (D), MYB43 (E), and MYB85 (F) bind to the promoter of *ADT6*. The cold probes used as competitors were with the same sequence as the TAMRA-labeled probes. Truncated MYB20 (Δ166–282 amino acids), MYB42 (Δ138–286 amino acids), MYB43 (Δ201–327 amino acids), and MYB85 (Δ168–266 amino acids) were used for yeast one-hybrid assay (A) and EMSA (C–F). G and H, Transient expression assays showed that the *ADT6* promoter can be activated by MYB20/42/43/85 in Arabidopsis Col-0 protoplasts (G) and in Arabidopsis *myb20/42/43/85* mutant protoplasts (H). CK was the empty vector used as a control and was set to 1. Data are means ± SD of three biological replicates. Based on Tukey's test, columns with the same letters are not significantly different and columns with different letters are significantly different ($P < 0.05$; one-way ANOVA).

evidence that MYB58/63 and MYB4 dynamically regulate lignin biosynthesis. MYB103, an NST1-regulated transcription factor, was recently suggested to be involved in syringyl lignin biosynthesis (Öhman et al., 2013). However, MYB103 did not directly target *F5H*, which is required for syringyl lignin formation (Öhman et al., 2013).

Phe derived from the shikimate pathway, which also gives rise to the other two aromatic amino acids Tyr and Trp, serves as a precursor for many secondary metabolites such as lignins, flavonoids, coumarins, and lignans (Maeda and Dudareva, 2012). Since lignin deposition is a very energy-consuming and nonreversible process, it is critical that Phe distribution among the phenylpropanoid pathway and protein synthesis is tightly controlled. AtMYB12 was previously shown to not only increase flavonoid biosynthesis but also to enhance the supply of precursors and carbon from primary metabolism (Zhang et al., 2015). It was also reported that a MYB transcription factor ODO1 from petunia was able to activate genes involved in the shikimate pathway and the biosynthesis of Phe-derived volatile compounds in tomato (Dal Cin et al., 2011). However, it remained unclear how plants coordinately regulate Phe formation in response to lignin biosynthesis.

It was previously shown that MYB85 was able to activate the expression of a lignin biosynthesis gene, *4CL1*, in a transient assay in Arabidopsis protoplasts (Zhong et al., 2008). In this study, we provided evidence that MYB85 and MYB42, along with MYB20 and MYB43, function as regulators of the lignin and shikimate biosynthesis pathways. MYB20, MYB42, MYB43, MYB85, MYB58, and MYB63 belong to a monophyletic

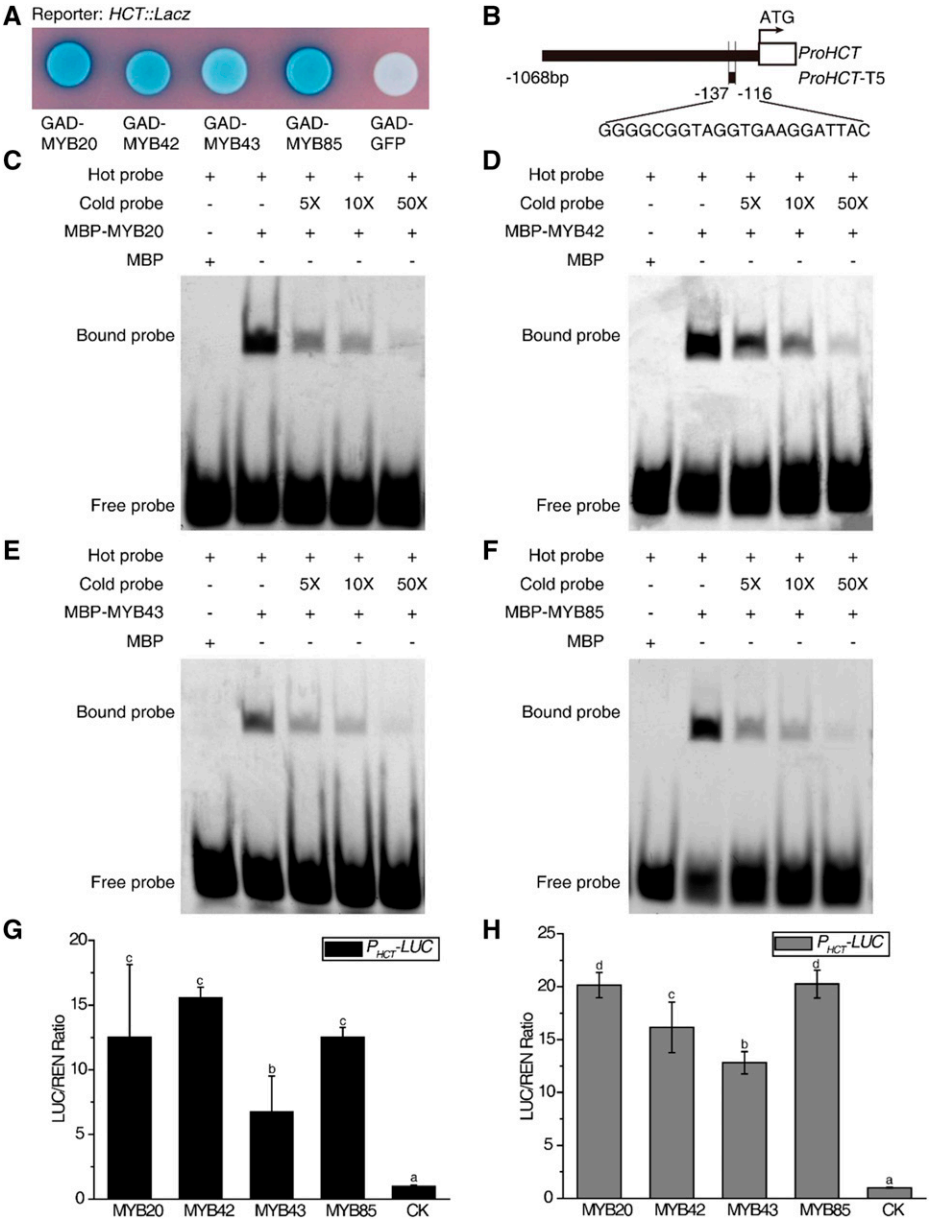

Figure 5. MYBs activate lignin biosynthesis genes. A, GAD-MYBs activate the expression of the *LacZ* reporter gene driven by the *HCT* promoter in yeast. GFP was used as the negative control. B, The top schematic diagram and the bottom one show the promoter regions of *HCT* in A and in C to F separately. C to F, EMSA showed that MYB20 (C), MYB42 (D), MYB43 (E), and MYB85 (F) bind to the promoter of *HCT*. The cold probes used as competitors were with the same sequence as the FAM-labeled probes. Truncated MYB20 (Δ166–282 amino acids), MYB42 (Δ138–286 amino acids), MYB43 (Δ201–327 amino acids), and MYB85 (Δ168–266 amino acids) were used for yeast one-hybrid assay (A) and EMSA (C–F). G and H, Transient expression assays showed that the *HCT* promoter can be activated by MYB20/42/43/85 in Arabidopsis Col-0 protoplasts (G) and in Arabidopsis *myb20/42/43/85* mutant protoplasts (H). CK was the empty vector used as a control and was set to 1. Data are means ± SD of three biological replicates. Based on Tukey's test, columns with the same letters are not significantly different and columns with different letters are significantly different ($P < 0.05$; one-way ANOVA).

group in the tree of MYB transcription factors, indicating that they have highly similar protein sequences (Supplemental Fig. S1). Among them, AtMYB20 and AtMYB43 have the highest similarity with AtMYB42 and AtMYB85 in Arabidopsis, forming a monophyletic clade with their putative orthologs in *Amborella trichopoda* and rice (*Oryza sativa*; Supplemental Fig. S1).

Disruption of *MYB20*, *MYB42*, *MYB43*, and *MYB85* significantly reduced the expression of genes involved in lignin biosynthesis (Fig. 3B). Consistent with gene reduction, lignin content was significantly reduced in *myb20/42/43/85* plants, indicating that MYB20, MYB42, MYB43, and MYB85 are regulators of lignin biosynthesis (Fig. 3D; Supplemental Fig. S4). Interestingly, *ADT* genes that are specifically involved in Phe biosynthesis were also down-regulated in *myb20/42/43/85* plants (Fig. 3A). However, free Phe content was increased despite the fact that *ADT* genes were down-regulated (Fig. 3C). This may be a consequence of down-regulated flux toward lignin biosynthesis. Even though Phe must be shunted toward enhanced flavonoid biosynthesis, it seems that lignin biosynthesis is down-regulated to a higher extent. Our data suggested that MYB20, MYB42, and MYB85 could directly target both lignin biosynthesis genes and *ADT* genes (Figs. 4A and 5A). However, MYB43 was only able to bind to the promoter of lignin biosynthesis genes, and not *ADT6*, in our yeast one-hybrid assay. EMSA data indicated that all four recombinant MBP-MYB fusion proteins caused an upshift of the labeled *ADT6* or *HCT* promoters. Interestingly, each MYB protein could activate *ADT* or lignin biosynthesis genes independently (Figs. 4G and 5G).

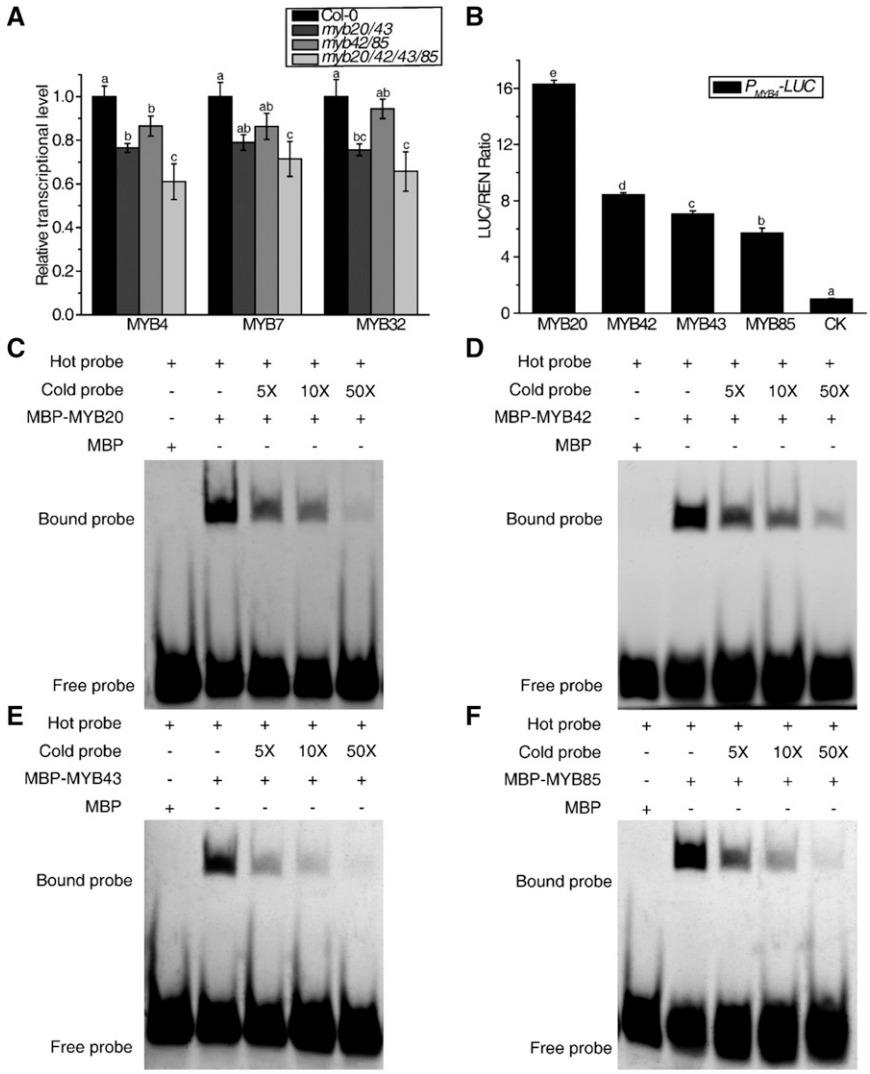

Figure 6. MYBs activate *MYB4/7/32* genes directly. A, *MYB4*, *MYB7*, and *MYB32* transcript levels in the inflorescence stems of 33-d-old wild-type, *myb20/43*, *myb42/85*, and *myb20/42/43/85* mutant plants as determined by RT-qPCR. B, Transient expression assays showed that the *MYB4* promoter can be activated by MYB20, MYB42, MYB43, and MYB85 in *N. benthamiana* leaves. CK was the vector of GUS-pEarleyGate 101, used as a control, and was set to 1. C to F, EMSA showed that MYB20 (C), MYB42 (D), MYB43 (E), and MYB85 (F) bind to the promoter of *MYB4*. The cold probes used as competitors were with the same sequence as the FAM-labeled probes. Truncated MYB20 (Δ166–282 amino acids), MYB42 (Δ138–286 amino acids), MYB43 (Δ201–327 amino acids), and MYB85 (Δ168–266 amino acids) were used for EMSA (C–F). Data are means ± SD of three biological replicates. Based on Tukey's test, columns with the same letters are not significantly different and columns with different letters are significantly different ($P < 0.05$; one-way ANOVA).

Like lignin, flavonoids are derived from Phe. Studies in Arabidopsis, as well as in maize, have pointed out that R2R3-MYBs have dual activation/repression effects on genes from flavonoid and lignin pathways that compete for carbon. For example, MYB32 and MYB4 in Arabidopsis were shown to influence the composition of the pollen wall by changing the flux through phenylpropanoid pathways (Preston et al., 2004). Similarly, Arabidopsis MYB75, a positive regulator of anthocyanin biosynthesis, was shown to regulate lignin accumulation negatively in secondary cell walls, which reflects carbon flux redistribution within the branches of phenylpropanoid metabolism (Bhargava et al., 2010). Overexpression of *ZmMYB31* from maize down-regulated several genes involved in monolignol biosynthesis and up-regulated flavonoid biosynthesis in Arabidopsis (Fornalé et al., 2010). However, it remains unclear how these MYBs fine-tune the biosynthesis of lignins and flavonoids. The channeling of carbon toward lignin and flavonoid pathways is thought to be highly coordinated by cross talk between these pathways. It was reported that AtMYB75 can interact with AtKNAT7, which functions as a negative regulator of secondary cell wall formation in interfascicular fibers (Bhargava et al., 2010; Wang et al., 2020a). A recent study further demonstrated that AtMYB4, a transcriptional repressor of lignin biosynthesis, along with its homologs MYB7 and MYB32, can attenuate the transcriptional function of MYB75-TT8-TTG1 complexes in flavonoid metabolism by interacting with the TT8 transcription factor (Wang et al., 2020b). The coordinated action of MYB repressors and activators has been proposed as a fine-tuning mechanism for the regulation of plant secondary metabolism (Bomal et al., 2014). In this study, we found that MYB20, MYB42, MYB43, and MYB85 redundantly activate *MYB4*, which was reported to repress the expression of *CHS*, which encodes the enzyme that catalyzes the first step of flavonoid biosynthesis. Consistent with the finding that the transcript level of *CHS* is enhanced in *myb20/42/43/85*, flavonoid biosynthesis is up-regulated in the mutant. In addition, MYB20 was shown to positively

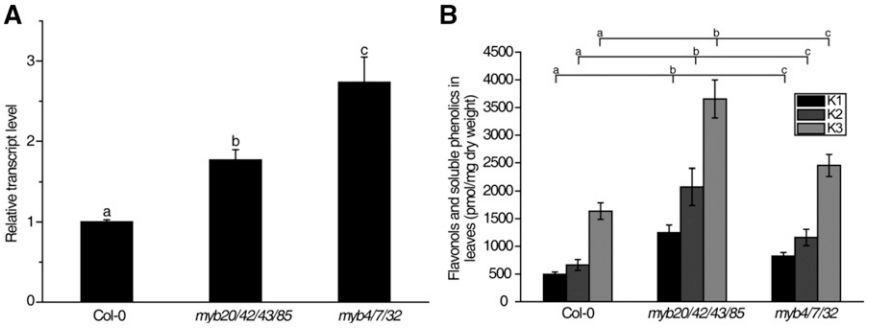

Figure 7. Disruption of *MYB20/42/43/85* promotes soluble flavonoid accumulation. A, RT-qPCR analysis of *CHS* in the inflorescence stems of 5-week-old wild-type, *myb20/42/43/85*, and *myb4/7/32* mutant plants. B, Quantification of the three major flavonols in the inflorescence stems of the same plants as in A. K1, Kaempferol 3-*O*-[6′′-*O*-(rhamnosyl)glucoside] 7-*O*-rhamnoside; K2, kaempferol 3-*O*-glucoside 7-*O*-rhamnoside; K3, kaempferol 3-*O*-rhamnoside 7-*O*-rhamnoside. Data are means ± SD of three biological replicates. Based on Tukey's test, columns with the same letters are not significantly different and columns with different letters are significantly different ($P < 0.05$; one-way ANOVA).

regulate the *CHS* promoter (Öhman et al., 2013), indicating that multiple levels of transcriptional control by MYB regulators can allow fine-tuned regulation of carbon flux along the phenylpropanoid pathway. In conclusion, our results showed that MYB20, MYB42, MYB43, and MYB85, in addition to positively regulating lignin biosynthesis by directly activating lignin and Phe biosynthesis genes, repress flavonoid accumulation through MYB4-mediated regulation of flavonoid biosynthesis. This suggests that the transcription factors MYB20, MYB42, MYB43, and MYB85 control carbon flow into the phenylpropanoid pathway by activating Phe biosynthesis to ensure precursor supply while at the same time repressing other competing metabolic pathways to optimize lignin biosynthesis. This discovery uncovers another level of complexity in the regulatory network of the plant lignin biosynthesis pathway.

MATERIALS AND METHODS

Plant Materials and Growth Conditions

The Arabidopsis (*Arabidopsis thaliana*) mutants *myb20-1* (GK-109C11-012312), *myb42-1* (SALKseq_78190.1), *myb43-1* (SALK_085312), *myb85-1* (SALK_052089), *nst1* (SALK_120377), and *nst3* (SALK_149909) were obtained from the Arabidopsis Biological Resource Center at Ohio State University. Seeds were sterilized with 3% (v/v) sodium hypochlorite, sown on one-half-strength Murashige and Skoog (MS) plates, stored at 4°C, and then transferred into a chamber under long-day conditions at 22°C (day/night cycle of 16/8 h). The primers used for genotyping are listed in Supplemental Table S1.

Phylogenetic Tree Analysis

Arabidopsis MYB20 was used as query to perform a BLASTP search against all genes annotated on 19 published genomes covering all main archaeplastida clades (Supplemental Table S2). Then, similar sequences with $E < 1e\text{-}3$ and an annotation term MYB transcription factors assigned by InterProScan (v5.24) were selected (Jones et al., 2014). Multiple protein sequence alignments of MYB transcription factors were performed using MAFFT (v7), and positions with more than 50% gaps were removed using the Phyutility program (v2.2.6; Smith and Dunn, 2008; Katoh and Standley, 2013). Phylogenetic analyses were performed with a maximum likelihood method by FastTree (v2.1) with optimal model of amino acid substitution (LG+G) chosen based on the results of ProtTest (v3.4.2), and a bootstrap analysis with 500 replicates was performed (Price et al., 2010; Darriba et al., 2011). Sequences belonging to the monophyletic group of Arabidopsis MYB20, MYB43, MYB42, MYB85, MYB58, and MYB63 were identified and selected for another round of phylogenetic analyses as described above. Only sequences annotated from Arabidopsis, rice (*Oryza sativa*), *Amborella trichopoda*, *Salvinia cucullata*, *Azolla filiculoides*, *Sphagnum fallax*, and *Physcomitrella patens* genomes were displayed on the final tree. Sequences with very atypical sizes and extremely long braches were manually removed.

Anthocyanin Measurement

Seedlings were grown on one-half strength MS medium containing 100 μM norflurazon. The seedlings were then grown for 4 d in a growth chamber. Photographs of the seedlings were taken by a microscope. To analyze anthocyanin content, the seeds were grown on plates with one-half strength MS medium containing 1% (w/v) Suc for 14 d and then transferred to one-half strength MS medium containing 12% (w/v) Suc for 3 d (Yonekura-Sakakibara et al., 2012). Plants were harvested and frozen with liquid nitrogen immediately. Anthocyanins were extracted with methanol containing 0.2% (v/v) formic acid and 30% (v/v) water and then placed at −20°C overnight to remove chlorophyll. The determination of anthocyanin content was carried out by spectrophotometry at 530 nm. The anthocyanin level of wild-type Col-0 (1.13 mg cyanidin 3-*O*-glucoside equivalence g^{-1}) was set to 100.

RNA Analyses

Total RNA was extracted from the inflorescence stems of 33-d-old Arabidopsis wild-type Col-0 and *myb20/42/43/85* mutants using the RNeasy Plant Mini Kit (Qiagen). Three biological replicates of each sample were sent to BGI Genomics (The Beijing Genomics Institute) for the construction of libraries and RNA sequencing. Data were analyzed on the Dr. Tom system from BGI.

The double mutants, *myb20/43* and *myb42/85*, were planted and harvested at the same time as wild-type Col-0 and the *myb20/42/43/85* mutant. Total RNA was reverse transcribed by Superscript Reverse Transcriptase III (Invitrogen). RT-qPCR was performed with SYBR Premix Ex Taq (Takara). The average levels of transcripts were from three biological replicates, and each biological replicate was from triplicate cDNA. The Arabidopsis *Tubulin* gene was used as a reference. The primers are listed in Supplemental Table S1.

KEGG Pathway Analysis

KEGG pathway enrichment analysis was performed using the Dr. Tom system from BGI. According to KEGG pathway annotation, phyper function in the R project was used to calculate *P* values and false discovery rates (FDRs).

Q value was the correction of the *P* value. Terms with $Q \leq 0.05$ were considered as enriched.

Dual-Luciferase Assay

To test transcriptional activation, the dual-luciferase assay was performed in *Nicotiana benthamiana* leaves. About 1 kb of the promoters of *MYB20*, *MYB42*, *MYB43*, *MYB85*, and *MYB4* was cloned into the pGreenII 0800-LUC vector to generate *P-LUC* reporter constructs (Hellens et al., 2005). Each promoter in pGreenII 0800-LUC was transformed into *Agrobacterium tumefaciens* strain GV3101 containing the helper plasmid pSoup-P19 (Hellens et al., 2005). The full-length coding sequences (without stop codons) of *NST3*, *MYB46*, *MYB20*, *MYB42*, *MYB43*, *MYB85*, and *GUS* were cloned into the pEarleyGate 101 vector. These six constructs were transformed into *A. tumefaciens* strain GV3101. Overnight cultures of *A. tumefaciens* strains were resuspended in infiltration buffer (10 mM $MgCl_2$, 10 mM MES, and 0.1 mM acetosyringone) to $OD_{600} \sim 0.6$ and incubated at room temperature for 2 h. The reporter:effector ratio was 2:8. Different combinations of *A. tumefaciens* suspension were infiltrated onto *N. benthamiana* leaves. After 48 h, leaf samples were collected and ground in liquid nitrogen for the dual-luciferase assay. Luciferase activities were detected using the Dual-Luciferase Reporter Assay System (Promega). Each sample contained three biological repeats.

To examine whether each MYB was able to activate the genes independently, a transcriptional activation assay was conducted in Arabidopsis Col-0 and *myb20/42/43/85* protoplasts. About 1 kb of promoters of *ADT6* and *HTC* was cloned into pGreenII 0800-LUC. The coding sequences of *MYB20*, *MYB42*, *MYB43*, and *MYB85* were inserted into p2GW7 under the control of the 35S promoter. After the protoplast preparation and subsequent transfection were completed (Yoo et al., 2007), samples were collected. The test of luciferase activities was described above. The raw data are given in Supplemental Table S3.

Yeast One-Hybrid Assays

GAD fusion constructs were cotransformed with the *LexAop::LacZ* (Clontech) reporter gene plasmid into the EGY48 yeast strain. Transformants were grown on appropriate dropout plates containing 5-bromo-4-chloro-3-indolyl-β-D-galactopyranoside for blue color test.

EMSA

The DNA fragments of MYBs were cloned into pMAL-c2x vector and expressed in the *Escherichia coli* BL21 (DE3) cell line, which were cultured in Luria-Bertani culture at 37°C to an OD_{600} between 0.6 and 0.8. To induce protein expression, a final concentration of 0.5 mM isopropyl β-D-1-thiogalactopyranoside was added to the cultures, after which the cells were incubated for 8 h at 28°C. Cells were harvested and resuspended in buffer containing 20 mM Tris-HCl, pH 7.4, 200 mM NaCl, and 1 mM EDTA, pH 8. After sonication and centrifugation, the MBP-TF proteins were purified using amylose resin from the supernatant.

The oligonucleotide probes were labeled with TAMRA or FAM and synthesized from Sangon Biotech. Then, the oligonucleotides were diluted to 10 μM, heated to 95°C for 5 min, and slowly cooled to room temperature. Briefly, 1 pmol of labeled probe was incubated with 0.1 μg of the indicated protein in 20 μL of reaction buffer (25 mM HEPES, pH 8, 40 mM KCl, 5 mM $MgCl_2$, 1 mM DTT, 1 mM EDTA, 8% [v/v] glycerol, and 1 μg of poly[dI-dC]) for 20 min at room temperature. Then, 5 μL of 5× loading buffer (12.5% [w/v] Ficoll-400, 0.2% [w/v] bromophenol blue, and 0.2% [w/v] xylene cyanol FF) was added to the reaction mixture and loaded onto a 4.5% polyacrylamide gel in 0.5× Tris-borate/EDTA. The labeled DNAs were detected using a Typhoon FLA 9500 Instrument (General Electric).

Amino Acid Extraction and Analysis

Amino acids were extracted from 50 mg (dry weight) of 5-week-old Arabidopsis stem samples with 1 mL of 0.5 M HCl solution. The supernatants were subsequently filtered using a 0.22-μm nylon membrane, and 250 μL of the extraction supernatant was transferred into autosamper vials. Finally, the mixture was diluted to 1 mL with 20% (v/v) water in acetonitrile prior to further analysis. Ultra-performance liquid chromatography (UPLC)-electrospray ionization-tandem mass spectrometry analysis was carried out on an Agilent 1290 LC system coupled to an Ultivo Triple Quadrupole mass spectrometer by means of an electrospray ionization probe. Eluent A was 20 mM ammonium formate in water (pH 3), while eluent B was 20 mM aqueous ammonium formate (pH 3) in 9:1 acetonitrile:water. The separation gradient was as follows: 100% B at 0 min, 70% B at 5 min, and 100% B at 8 min. The column temperature was maintained at 25°C. The injection volume of each sample was 1 μL. The multiple reaction monitoring mass spectrometry method was employed for the quantitation of amino acids. Data for Phe were acquired in positive ion mode under the following operating conditions: desolvation temperature, 330°C; desolvation gas (N_2) rate, 13 L min^{-1}; collision energy, 13 V for quantitative ion (mass-to-charge ratio [*m/z*] 120.1) and 29 V for qualitative ion (*m/z* 103).

Determination of Lignin Composition

Thioacidolysis analysis was performed to determine lignin composition. Briefly, 30-mg samples were reacted with 3 mL of 0.2 M BF_3-etherate in an 8.75:1 dioxane:ethanethiol mixture at 100°C for 4 h. After adding 4 mL of water, the mixture was extracted using 4 mL of dichloromethane (three times). The organic layer was separated and dried under a stream of nitrogen. After derivatization with *N*,*O*-bis-(trimethylsilyl)trifluoroacetamide + 1% (w/v) trimethylchlorosilane (Sigma-Aldrich), lignin-derived monomers were identified by GC-mass spectrometry and quantified by GC as their trimethylsilyl derivatives. GC-mass spectrometry was performed on an Agilent Intuvo 9000 GC system with a 5977B series mass selective detector (column, HP-5MS; 30 m × 0.25 mm; 0.25-μm film thickness), and mass spectra were recorded in electron impact mode (70 eV) with a 50 to 650 *m/z* scanning range.

Quantification of Flavonoids

Samples of three replicates of Arabidopsis stems were collected and ground into a fine powder with a mortar and pestle under liquid nitrogen. Twenty-microgram dried samples were extracted with 1 mL of 80% (v/v) methanol (containing 100 μM naringenin as an internal reference), and then ultrasonic processing was conducted for 30 min at room temperature. After that, the samples were centrifuged at 14,000*g* for 10 min, and the supernatant was transferred to a sterile 1.5-mL Eppendorf tube for another centrifugation as above. A total of 300 μL of sterile Milli-Q water was added to each 1-mL supernatant solution and stored at −20°C overnight to precipitate chlorophyll. The following day, 5 μL of the supernatant solution after another centrifugation was injected for UPLC analysis. The identification of soluble flavonoid compounds was described previously (Yonekura-Sakakibara et al., 2008), and quantification of detected compounds was based on the standard curves of a kaempferol standard detected in the same UPLC runs.

Statistical Analyses

The SPSS 20.0 statistical package (IBM SPSS Statistics for Windows, Version 20.0; IBM Corp) was used for the statistical data analysis. Statistical analysis was done with univariate analysis and Scheffe posthoc testing at the 5% level. Samples included in the analysis were arranged based on at least three biological replicates.

Data Availability

RNA sequencing data have been uploaded to the Sequence Read Archive (http://www.ncbi.nlm.nih.gov/sra) with the accession number PRJNA578015.

Accession Numbers

The Arabidopsis Information Resource accession numbers of genes mentioned are as follows: AT2G46770 (*NST1*), AT3G61910 (*NST2*), AT1G32770 (*NST3*), AT5G12870 (*MYB46*), AT1G66230 (*MYB20*), AT4G12350 (*MYB42*), AT5G16600 (*MYB43*), AT4G22680 (*MYB85*), AT4G38620 (*MYB4*), AT2G16720 (*MYB7*), AT4G34990 (*MYB32*), AT2G37040 (*PAL1*), AT2G30490 (*C4H*), AT1G15710 (*ADH2*), AT3G44720 (*ADT4*), AT5G22630 (*ADT5*), AT1G08250 (*ADT6*), AT1G51680 (*4CL1*), AT3G19450 (*CAD4*), AT1G52760 (*CSE*), AT5G48930 (*HCT*), AT3G54640 (*TSA1*), AT5G54810 (*TSB1*), and AT5G13930 (*CHS*).

Supplemental Data

The following supplemental materials are available.

Supplemental Figure S1. Phylogenetic tree analysis of MYBs in 19 published genomes in main archaeplastida clades.

Supplemental Figure S2. NST1/2/3 and MYB46/83 could not bind the promoters of *MYB20/42/43/85* directly.

Supplemental Figure S3. KEGG pathway enrichment analysis.

Supplemental Figure S4. Lignin content Klason analysis of the wild type (Col-0), *myb20/43*, *myb42/85*, and *myb20/42/43/85*.

Supplemental Figure S5. Truncated MYB proteins have higher expression in yeast.

Supplemental Figure S6. Disruption of *MYB20/42/43/85* promotes anthocyanin accumulation.

Supplemental Table S1. Primers used for vector construction and gene expression analysis.

Supplemental Table S2. Resources of 19 representative genomes used in phylogenetic tree analysis.

Supplemental Table S3. Source data of the firefly and *Renilla* luciferase signal in the dual-luciferase assay.

Supplemental Data Set S1. A full list of the genes that are up-regulated in *myb20/42/43/85* (FDR < 0.05, $\log_2$ fold change > 1).

Supplemental Data Set S2. A full list of the genes that are down-regulated in *myb20/42/43/85* (FDR < 0.05, $\log_2$ fold change < -1).

Received September 5, 2019; accepted December 9, 2019; published December 23, 2019.

LITERATURE CITED

Bhargava A, Mansfield SD, Hall HC, Douglas CJ, Ellis BE (2010) MYB75 functions in regulation of secondary cell wall formation in the Arabidopsis inflorescence stem. Plant Physiol **154:** 1428–1438

Bomal C, Duval I, Giguère I, Fortin É, Caron S, Stewart D, Boyle B, Séguin A, MacKay JJ (2014) Opposite action of R2R3-MYBs from different subgroups on key genes of the shikimate and monolignol pathways in spruce. J Exp Bot **65:** 495–508

Bonawitz ND, Chapple C (2010) The genetics of lignin biosynthesis: Connecting genotype to phenotype. Annu Rev Genet **44:** 337–363

Chen F, Tobimatsu Y, Havkin-Frenkel D, Dixon RA, Ralph J (2012) A polymer of caffeyl alcohol in plant seeds. Proc Natl Acad Sci USA **109:** 1772–1777

Chen F, Tobimatsu Y, Jackson L, Nakashima J, Ralph J, Dixon RA (2013) Novel seed coat lignins in the Cactaceae: Structure, distribution and implications for the evolution of lignin diversity. Plant J **73:** 201–211

Cosgrove DJ, Jarvis MC (2012) Comparative structure and biomechanics of plant primary and secondary cell walls. Front Plant Sci **3:** 204

Dal Cin V, Tieman DM, Tohge T, McQuinn R, de Vos RC, Osorio S, Schmelz EA, Taylor MG, Smits-Kroon MT, Schuurink RC, et al (2011) Identification of genes in the phenylalanine metabolic pathway by ectopic expression of a MYB transcription factor in tomato fruit. Plant Cell **23:** 2738–2753

Darriba D, Taboada GL, Doallo R, Posada D (2011) ProtTest 3: Fast selection of best-fit models of protein evolution. Bioinformatics **27:** 1164–1165

Fornalé S, Shi X, Chai C, Encina A, Irar S, Capellades M, Fuguet E, Torres JL, Rovira P, Puigdomènech P, et al (2010) ZmMYB31 directly represses maize lignin genes and redirects the phenylpropanoid metabolic flux. Plant J **64:** 633–644

Fraser CM, Chapple C (2011) The phenylpropanoid pathway in Arabidopsis. The Arabidopsis Book **9:** e0152

Goicoechea M, Lacombe E, Legay S, Mihaljevic S, Rech P, Jauneau A, Lapierre C, Pollet B, Verhaegen D, Chaubet-Gigot N, et al (2005) *Eg*MYB2, a new transcriptional activator from *Eucalyptus xylem*, regulates secondary cell wall formation and lignin biosynthesis. Plant J **43:** 553–567

Hellens RP, Allan AC, Friel EN, Bolitho K, Grafton K, Templeton MD, Karunairetnam S, Gleave AP, Laing WA (2005) Transient expression vectors for functional genomics, quantification of promoter activity and RNA silencing in plants. Plant Methods **1:** 13

Hoson T, Wakabayashi K (2015) Role of the plant cell wall in gravity resistance. Phytochemistry **112:** 84–90

Jin H, Cominelli E, Bailey P, Parr A, Mehrtens F, Jones J, Tonelli C, Weisshaar B, Martin C (2000) Transcriptional repression by AtMYB4 controls production of UV-protecting sunscreens in *Arabidopsis*. EMBO J **19:** 6150–6161

Jones P, Binns D, Chang HY, Fraser M, Li W, McAnulla C, McWilliam H, Maslen J, Mitchell A, Nuka G, et al (2014) InterProScan 5: Genome-scale protein function classification. Bioinformatics **30:** 1236–1240

Katoh K, Standley DM (2013) MAFFT multiple sequence alignment software version 7: Improvements in performance and usability. Mol Biol Evol **30:** 772–780

Kim WC, Kim JY, Ko JH, Kang H, Han KH (2014) Identification of direct targets of transcription factor MYB46 provides insights into the transcriptional regulation of secondary wall biosynthesis. Plant Mol Biol **85:** 589–599

Kim WC, Kim JY, Ko JH, Kim J, Han KH (2013a) Transcription factor MYB46 is an obligate component of the transcriptional regulatory complex for functional expression of secondary wall-associated cellulose synthases in Arabidopsis thaliana. J Plant Physiol **170:** 1374–1378

Kim WC, Ko JH, Han KH (2012) Identification of a *cis*-acting regulatory motif recognized by MYB46, a master transcriptional regulator of secondary wall biosynthesis. Plant Mol Biol **78:** 489–501

Kim WC, Ko JH, Kim JY, Kim J, Bae HJ, Han KH (2013b) MYB46 directly regulates the gene expression of secondary wall-associated cellulose synthases in Arabidopsis. Plant J **73:** 26–36

Ko JH, Jeon HW, Kim WC, Kim JY, Han KH (2014) The MYB46/MYB83-mediated transcriptional regulatory programme is a gatekeeper of secondary wall biosynthesis. Ann Bot **114:** 1099–1107

Kubo M, Udagawa M, Nishikubo N, Horiguchi G, Yamaguchi M, Ito J, Mimura T, Fukuda H, Demura T (2005) Transcription switches for protoxylem and metaxylem vessel formation. Genes Dev **19:** 1855–1860

Legay S, Sivadon P, Blervacq AS, Pavy N, Baghdady A, Tremblay L, Levasseur C, Ladouce N, Lapierre C, Séguin A, et al (2010) *Eg*MYB1, an R2R3 MYB transcription factor from eucalyptus negatively regulates secondary cell wall formation in *Arabidopsis* and poplar. New Phytol **188:** 774–786

Li M, Li Y, Guo L, Gong N, Pang Y, Jiang W, Liu Y, Jiang X, Zhao L, Wang Y, et al (2017) Functional characterization of tea (*Camellia sinensis*) MYB4a transcription factor using an integrative approach. Front Plant Sci **8:** 943

Li Z, Omranian N, Neumetzler L, Wang T, Herter T, Usadel B, Demura T, Giavalisco P, Nikoloski Z, Persson S (2016) A transcriptional and metabolic framework for secondary wall formation in Arabidopsis. Plant Physiol **172:** 1334–1351

Maeda H, Dudareva N (2012) The shikimate pathway and aromatic amino acid biosynthesis in plants. Annu Rev Plant Biol **63:** 73–105

Maeda H, Shasany AK, Schnepp J, Orlova I, Taguchi G, Cooper BR, Rhodes D, Pichersky E, Dudareva N (2010) RNAi suppression of *Arogenate Dehydratase1* reveals that phenylalanine is synthesized predominantly via the arogenate pathway in petunia petals. Plant Cell **22:** 832–849

McCarthy RL, Zhong R, Ye ZH (2009) MYB83 is a direct target of SND1 and acts redundantly with MYB46 in the regulation of secondary cell wall biosynthesis in Arabidopsis. Plant Cell Physiol **50:** 1950–1964

Mitsuda N, Iwase A, Yamamoto H, Yoshida M, Seki M, Shinozaki K, Ohme-Takagi M (2007) NAC transcription factors, NST1 and NST3, are key regulators of the formation of secondary walls in woody tissues of *Arabidopsis*. Plant Cell **19:** 270–280

Mitsuda N, Seki M, Shinozaki K, Ohme-Takagi M (2005) The NAC transcription factors NST1 and NST2 of *Arabidopsis* regulate secondary wall thickenings and are required for anther dehiscence. Plant Cell **17:** 2993–3006

Öhman D, Demedts B, Kumar M, Gerber L, Gorzsás A, Goeminne G, Hedenström M, Ellis B, Boerjan W, Sundberg B (2013) MYB103 is required for *FERULATE-5-HYDROXYLASE* expression and syringyl lignin biosynthesis in Arabidopsis stems. Plant J **73:** 63–76

Ohtani M, Demura T (2019) The quest for transcriptional hubs of lignin biosynthesis: Beyond the NAC-MYB-gene regulatory network model. Curr Opin Biotechnol **56:** 82–87

Ohtani M, Morisaki K, Sawada Y, Sano R, Uy ALT, Yamamoto A, Kurata T, Nakano Y, Suzuki S, Matsuda M, et al (2016) Primary metabolism during biosynthesis of secondary wall polymers of protoxylem vessel elements. Plant Physiol **172:** 1612–1624

Patzlaff A, McInnis S, Courtenay A, Surman C, Newman LJ, Smith C, Bevan MW, Mansfield S, Whetten RW, Sederoff RR, et al (2003) Characterisation of a pine MYB that regulates lignification. Plant J **36:** 743–754

Preston J, Wheeler J, Heazlewood J, Li SF, Parish RW (2004) AtMYB32 is required for normal pollen development in *Arabidopsis thaliana*. Plant J **40:** 979–995

Price MN, Dehal PS, Arkin AP (2010) FastTree 2: Approximately maximum-likelihood trees for large alignments. PLoS ONE **5:** e9490

Qian Y, Lynch JH, Guo L, Rhodes D, Morgan JA, Dudareva N (2019) Completion of the cytosolic post-chorismate phenylalanine biosynthetic pathway in plants. Nat Commun **10:** 15

Raes J, Rohde A, Christensen JH, Van de Peer Y, Boerjan W (2003) Genome-wide characterization of the lignification toolbox in Arabidopsis. Plant Physiol **133:** 1051–1071

Shen H, He X, Poovaiah CR, Wuddineh WA, Ma J, Mann DG, Wang H, Jackson L, Tang Y, Stewart CN Jr., et al (2012) Functional characterization of the switchgrass (*Panicum virgatum*) R2R3-MYB transcription factor *PvMYB4* for improvement of lignocellulosic feedstocks. New Phytol **193:** 121–136

Smith SA, Dunn CW (2008) Phyutility: A phyloinformatics tool for trees, alignments and molecular data. Bioinformatics **24:** 715–716

Tamagnone L, Merida A, Parr A, Mackay S, Culianez-Macia FA, Roberts K, Martin C (1998) The AmMYB308 and AmMYB330 transcription factors from Antirrhinum regulate phenylpropanoid and lignin biosynthesis in transgenic tobacco. Plant Cell **10:** 135–154

Tohge T, Watanabe M, Hoefgen R, Fernie AR (2013) Shikimate and phenylalanine biosynthesis in the green lineage. Front Plant Sci **4:** 62

Wang S, Yamaguchi M, Grienenberger E, Martone PT, Samuels AL, Mansfield SD (2020a) The class II KNOX genes KNAT3 and KNAT7 work cooperatively to influence deposition of secondary cell walls that provide mechanical support to Arabidopsis stems. Plant J **101:** 293–309

Wang XC, Wu J, Guan ML, Zhao CH, Geng P, Zhao Q (2020b) *Arabidopsis* MYB4 plays dual roles in flavonoid biosynthesis. Plant J **101:** 637–652

Weng JK, Mo H, Chapple C (2010) Over-expression of F5H in COMT-deficient Arabidopsis leads to enrichment of an unusual lignin and disruption of pollen wall formation. Plant J **64:** 898–911

Yonekura-Sakakibara K, Fukushima A, Nakabayashi R, Hanada K, Matsuda F, Sugawara S, Inoue E, Kuromori T, Ito T, Shinozaki K, et al (2012) Two glycosyltransferases involved in anthocyanin modification delineated by transcriptome independent component analysis in *Arabidopsis thaliana*. Plant J **69:** 154–167

Yonekura-Sakakibara K, Tohge T, Matsuda F, Nakabayashi R, Takayama H, Niida R, Watanabe-Takahashi A, Inoue E, Saito K (2008) Comprehensive flavonol profiling and transcriptome coexpression analysis leading to decoding gene-metabolite correlations in *Arabidopsis*. Plant Cell **20:** 2160–2176

Yoo H, Widhalm JR, Qian Y, Maeda H, Cooper BR, Jannasch AS, Gonda I, Lewinsohn E, Rhodes D, Dudareva N (2013) An alternative pathway contributes to phenylalanine biosynthesis in plants via a cytosolic tyrosine:phenylpyruvate aminotransferase. Nat Commun **4:** 2833

Yoo SD, Cho YH, Sheen J (2007) *Arabidopsis* mesophyll protoplasts: A versatile cell system for transient gene expression analysis. Nat Protoc **2:** 1565–1572

Zhang Y, Butelli E, Alseekh S, Tohge T, Rallapalli G, Luo J, Kawar PG, Hill L, Santino A, Fernie AR, et al (2015) Multi-level engineering facilitates the production of phenylpropanoid compounds in tomato. Nat Commun **6:** 8635

Zhao J, Zhang W, Zhao Y, Gong X, Guo L, Zhu G, Wang X, Gong Z, Schumaker KS, Guo Y (2007) SAD2, an importin-like protein, is required for UV-B response in Arabidopsis by mediating MYB4 nuclear trafficking. Plant Cell **19:** 3805–3818

Zhao Q (2016) Lignification: Flexibility, biosynthesis and regulation. Trends Plant Sci **21:** 713–721

Zhao Q, Dixon RA (2014) Altering the cell wall and its impact on plant disease: From forage to bioenergy. Annu Rev Phytopathol **52:** 69–91

Zhao Q, Tobimatsu Y, Zhou R, Pattathil S, Gallego-Giraldo L, Fu C, Jackson LA, Hahn MG, Kim H, Chen F, et al (2013) Loss of function of cinnamyl alcohol dehydrogenase 1 leads to unconventional lignin and a temperature-sensitive growth defect in *Medicago truncatula*. Proc Natl Acad Sci USA **110:** 13660–13665

Zhong R, Lee C, Ye ZH (2010) Global analysis of direct targets of secondary wall NAC master switches in *Arabidopsis*. Mol Plant **3:** 1087–1103

Zhong R, Lee C, Zhou J, McCarthy RL, Ye ZH (2008) A battery of transcription factors involved in the regulation of secondary cell wall biosynthesis in *Arabidopsis*. Plant Cell **20:** 2763–2782

Zhong R, Ye ZH (2012) MYB46 and MYB83 bind to the SMRE sites and directly activate a suite of transcription factors and secondary wall biosynthetic genes. Plant Cell Physiol **53:** 368–380

Zhou J, Lee C, Zhong R, Ye ZH (2009) MYB58 and MYB63 are transcriptional activators of the lignin biosynthetic pathway during secondary cell wall formation in *Arabidopsis*. Plant Cell **21:** 248–266